Eur. J. Biochem. *143*, 221 – 226 (1984)
© FEBS 1984

Metabolic resistance to tight-binding inhibitors of enzymes involved in the *de novo* pyrimidine pathway

Simulation of time-dependent effects

Ronald G. DUGGLEBY and Richard I. CHRISTOPHERSON

Department of Biochemistry, University of Queensland, St Lucia; and
Department of Biochemistry, University of Melbourne, Parkville

(Received April 4, 1984) – EJB 84 0349

When a tight-binding inhibitor interacts with a target enzyme of a metabolic pathway, the end products of the pathway are depleted and the substrate(s) for the inhibited reaction accumulate. The accumulating substrate(s) can reach a concentration which is sufficiently high that the inhibition is effectively reversed, with restoration of the original flux through the inhibited reaction. We have recently developed a theoretical model for this phenomenon which we have called 'metabolic resistance' [R. I. Christopherson and R. G. Duggleby (1983) *Eur. J. Biochem. 134*, 331 – 335].

In the present communication, we have successfully used the technique of numerical integration to simulate the effects of inhibition of several enzymes in the pathway of pyrimidine biosynthesis. Utilizing appropriate dissociation constants and enzyme concentrations for the inhibited systems, these simulations are consistent with published experimental data for the interactions of *N*-phosphonacetyl-L-aspartate (*P*AcAsp) with mammalian aspartate transcarbamoylase *in vitro* [R. I. Christopherson and M. E. Jones (1980) *J. Biol. Chem. 255*, 11381 – 11395] and of 5-fluorodeoxyuridine 5′-phosphate (FdUMP) with thymidylate synthetase *in vivo* [R. G. Moran, C. P. Spears, and C. Heidelberger (1979) *Proc. Natl Acad. Sci. USA 76*, 1456 – 1460]. In addition, we present a simulation of the expected effect *in vivo* of phosphoribofuranosyl barbituric acid (BMP), a tight-binding inhibitor of OMP decarboxylase [H. L. Levine, R. S. Brody, and F. H. Westheimer (1980) *Biochemistry 19*, 4993 – 4999]. This simulation shows that on addition of BMP, there is a sequential depletion of all pyrimidine intermediates between UMP and dCDP and a concomitant accumulation of OMP. Eventually, OMP reaches a new steady-state concentration and the concentrations of the depleted intermediates rise to their original levels. We have simulated the depletion of dCDP at various concentrations of BMP; since dCDP is comitted to DNA synthesis we can integrate the dCDP concentrations over time to calculate the amount of DNA synthesis and thereby predict the delay in cell division which would be elicited by BMP. This form of analysis may help to explain in quantitative terms why inhibitors of nucleic acid biosynthesis have a selective toxicity for rapidly growing tumour cells.

Of the approximately 85 enzymic reactions involved in the biosynthesis of pyrimidine and purine nucleotides via the *de novo* and salvage pathways and their subsequent polymerizations to nucleic acids, approximately 14 of the enzymes can be inhibited by metabolite analogues [1] which have a selective toxicity for rapidly growing cancer cells because of their more rapid rate of nucleic acid biosynthesis, relative to normal cells. The catalytic mechanisms of many of the enzymes involved in nucleic acid biosynthesis are now well understood which in turn enables rational design of potential tight-binding inhibitors of these pathways, with potential therapeutic value.

Theory and techniques for the quantitative analysis of the interaction of a tight-binding inhibitor with a purified target enzyme *in vitro* have been established (see [2]). An equally important objective is to relate quantitative information obtained *in vitro* to the interaction of a tight-binding inhibitor with a target enzyme of a functioning metabolic pathway in a growing cell. In a previous paper [3] we described a phenomenon called 'metabolic resistance' and from an appropriate theroetical model we were able to make quantitative predictions about the new steady-state which would be reached in a metabolic pathway as a consequence of tight-binding inhibition of one of the constituent reactions. For all such systems metabolic resistance can arise when the substrate of the inhibited enzyme accumulates to a concentration sufficient to reverse the inhibition, provided that the accumulating substrate is not removed by some other process.

In cancer chemotherapy it is not only the final steady-state condition of metabolic resistance which is important; the time course for depletion and subsequent recovery of the end products of the pathway may contribute to the therapeutic effect. In the treatment of cancer with methotrexate, a tight-binding inhibitor of dihydrofolate reductase, a strategy of 'thymidine rescue' has been developed [4] which is designed to

Abbreviations. *P*AcAsp, *N*-phosphonacetyl-L-aspartate; BMP, 1-(5′-phospho-β-D-ribofuranosyl)barbituric acid; FUra, 5-fluorouracil; FdUMP, 5-fluorodeoxyuridine 5′-monophosphate; Cbm-*P*, carbamoyl phosphate; CbmAsp, *N*-carbamoyl-L-aspartate; hOro, L-5,6-dihydroorotate; Oro, orotate; *P*-Rib-*PP*, 5-phosphoribosyl-1-diphosphate.

Enzymes. Carbamoyl phosphate synthetase (EC 6.3.5.5); aspartate transcarbamoylase (EC 2.1.3.2); dihydroorotase (EC 3.5.2.3); orotate phosphoribosyltransferase (EC 2.4.2.10); OMP decarboxylase (EC 4.1.1.23); nucleoside diphosphate kinase (EC 2.7.4.6); CTP synthetase (EC 6.3.4.2); ribonucleotide reductase (EC 1.17.4.1); thymidylate synthetase (EC 2.1.1.45).

cause the death of rapidly growing cancer cells while eventually rescuing the patient from the potentially lethal effects of a deficiency of dTTP. Clearly, in this situation, the progress curves for depletion of nucleic acid precursors after drug administration could be vital for timing the rescue procedure. In this paper we simulate such progress curves for two interactions of a tight-binding inhibitor with its target enzyme using the technique of numerical integration. This technique is then applied to simulate the expected effect on the pyrimidine pathway of phosphoribofuranosyl barbituric acid (BMP), a tight-binding inhibitor of OMP decarboxylase.

THEORY AND SIMULATION PROCEDURES

We have recently developed a theoretical model for metabolic resistance where interaction of a tight-binding inhibitor with a target enzyme of a metabolic pathway results in accumulation of the substrate of that enzyme and ultimately in full restoration of enzymic activity [3]. This analysis of metabolic resistance compared the initial uninhibited steady-state concentration of substrate with its final steady-state concentration after addition of inhibitor. It is also possible to predict the progress curves for the concentrations of substrate(s) and product(s) between the initial and final steady states as a function of time and the relevant theory will be outlined here.

Consider the arbitrary metabolic sequence

$$X_0 \xrightarrow{v_0} X_1 \xrightarrow{E_1} X_2 \xrightarrow{E_2} X_3 \xrightarrow{E_3} \text{etc.}$$

in which a precursor (X_0) is being converted to an intermediate (X_1) at a constant rate, v_0. An enzyme (E_1) converts X_1 to a second intermediate (X_2) which is itself converted to X_3 by E_2, and so on. Given that the enzymes involved show simple Michaelis-Menten kinetics and that the maximum velocity and Michaelis constant of each is known, we may write a differential equation for the concentration of the jth intermediate, X_j, at any time:

$$\frac{d[X_j]}{dt} = v_{j-1} - v_j \tag{2a}$$

where

$$v_j = \frac{V_j[X_j]}{K_j + [X_j]} \tag{2b}$$

and the symbols V_j and K_j represent the maximum velocity and Michaelis constant, respectively, of the enzyme E_j. Given a value for v_0, this system of differential equations is readily solved to yield the steady-state concentration of each intermediate. Alternatively, if the steady-state concentrations and Michaelis constants are known, the maximum velocities may be calculated.

If such a system is now perturbed by adding a competitive inhibitor (I) of E_1, v_1 will decrease:

$$v_1 = \frac{V_1[X_1]}{K_1(1 + [I]/K_i) + [X_1]}. \tag{3}$$

As a consequence, the system will no longer be at steady state; there will be an immediate decrease in the concentration of X_2 and a delayed decline in that of X_3 and subsequent intermediates. Meanwhile, X_1 will rise and as it does so it will begin to reverse the inhibition. Eventually, X_1 will have risen sufficiently to restore the steady-state condition, $v_1 = v_0$, and all intermediates downstream of the inhibited step will be restored to their original levels. The new steady-state concentration of X_1 may be calculated as before but if we wish to follow the time course of the approach to this new steady state we may do so by numerical integration of the relevant differential equations. In the work described here, numerical integration was performed using a computer program which was written in FORTRAN and which uses a fourth-order Runge-Kutta method [5]. The integration routine was taken from the CRICF program [6].

Eq (3) describes the effect of a classical competitive inhibitor. For a tight-binding inhibitor, the situation is much the same except that the definition of v_1 will be more complex and will require a distinction to be drawn between free concentration of inhibitor[I] and total inhibitor concentration $[I]_T$ and will also require a knowledge of the total enzyme concentration, $[E]_T$. Specifically, v_1, is given by:

$$v_1 = \frac{V_1[X_1]}{2[E]_T(K_1 + [X_1])}\left[-Q + (Q^2 + 4K_i'[E]_T)^{\frac{1}{2}}\right] \tag{4a}$$

where

$$Q = K_i' + [I]_T - [E]_T \tag{4b}$$

and

$$K_i' = K_i(1 + [X_1]/K_1). \tag{4c}$$

Several tight-binding inhibitors also exhibit slow-binding characetristics and under these circumstances an explicit expression for v_1 cannot be written down. Rather, a set of equations must be introduced to describe the variation of the concentration of the enzyme-inhibitor complex (EI) with time.

$$[E] = \frac{[E]_T - [EI]}{1 + [X_1]/K_1} \tag{5a}$$

$$[I] = [I]_T - [EI] \tag{5b}$$

$$\frac{d[EI]}{dt} = k_3[E][I] - k_4[EI] \tag{5c}$$

$$v_1 = \frac{V_1(1 - [EI]/[E]_T)}{1 + K_1/[X_1]} \tag{5d}$$

In Eq. (5c), k_3 and k_4 represent the rate constants for formation and dissociation, respectively, of EI and are related to the inhibition constant by the relationship: $K_i = k_4/k_3$.

The general approach described above was used in all of the simulations which are discussed later. Specific details relating to individual systems are noted at the appropriate places in the text.

RESULTS AND DISCUSSION

Tight-binding inhibition of an enzyme of the *de novo* pyrimidine pathway will ultimately result in depletion of the nucleoside triphosphate end-products of the pathway: UTP, CTP, dCTP and dTTP. It has been suggested by several laboratories that the pool size of certain deoxyribonucleoside triphosphates may have a regulatory function for the rate of DNA synthesis (e.g. [7,8]). We have therefore obtained from the literature approximate intracellular concentrations for the intermediates of this pathway as well as the apparent Michaelis constants and V values for enzymes of the pyrimidine pathway leading from HCO_3^- to CDP (Table 1). It is noteworthy that the three enzymes with the lowest V values in the sequence are carbamoyl phosphate synthetase, CTP synthetase and ribonucleotide reductase and that only these enzymes are subject to

Table 1. *Cellular concentrations of pyrimidine pathway intermediates and their kinetic constants*
Michaelis constants (K_m) and maximum velocities (V) are listed for each intermediate acting as a substrate for the enzyme catalysing the succeeding reaction in the metabolic sequence from HCO_3^- to CDP. Values for V are for a crude cell-free extract

Pyrimidine intermediate	Cellular concentration		K_m		V	
	μM		μM		nmol min^{-1} (mg protein)$^{-1}$	
HCO_3^-	24000	[9]	610	[10]	0.32	[10][a]
Cbm-*P*	0.2	[10]	22.1	[3]	18	[10][a]
CbmAsp	7.1	[10]	260	[10]	2.8	[10][a]
hOro	—[b]		5.2	[11]	1.0	[11]
Oro	0.4	[12]	2.0	[13]	1.5	[11]
OMP	0.07	[12]	0.23	[13]	2.2	[11]
UMP	19	[14][c]	43	[15]	170	[16]
UDP	39	[14][c]	200	[17][d]	4400	[16]
UTP	1000	[11]	25	[18]	0.005	[18]
CTP	515	[14][c]	—[b]		—[b]	
CDP	10	[14][c]	30	[19]	0.078	[20]

[a] Calculated from [10] using the ratio of maximal activities of hOro synthetase for carbamoyl phosphate synthetase:aspartate transcarbamoylase:dihydroorotase of 1.0:57:8.8 for the purified synthetase and the specific activity for aspartate transcarbamoylase of a cell-free extract of mouse Ehrlich ascites tumour cells of 18.1 pmol min^{-1} (μg protein)$^{-1}$.

[b] An appropriate value was not available.

[c] Calculated by ratio from [14] by assuming that a cellular UTP level of 2390 pmol/10^6 cells [14] is equivalent to a UTP concentration of 1.0 mM [11].

[d] A Michaelis constant of UDP for nucleoside diphosphate kinase was unavailable and an average value for CDP [17] of 200 μM is listed.

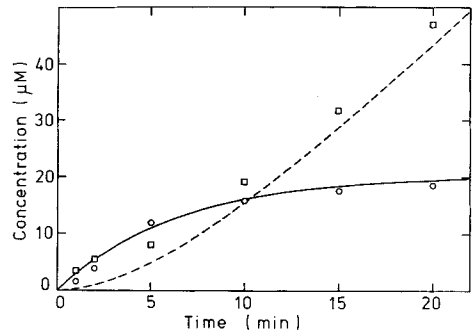

Fig. 1. *Simulation of progress curves for Cbm-*P *and CbmAsp when aspartate transcarbamoylase is inhibited by 0.8 μM* P*AcAsp.* Experimental values plotted for the concentration of Cbm-*P* (○) and total CbmAsp synthesized (□) are from [10]. The simulation was performed using the following parameter values [3]: initial Cbm-*P* concentration, 0.202 μM; apparent Michaelis constant for Cbm-*P*, 22.1 μM; total concentration of hOro synthetase, 0.093 μM; turnover number of aspartate transcarbamoylase, 3720 min^{-1}; inhibition constant for *P*AcAsp, 6.2 nM; and half-life for decomposition of Cbm-*P*, 37.6 min [10]. Details are described in the theoretical section of this paper

allosteric regulation which could substantially change these unregulated V values (Table 1) *in vivo*. Carbamoyl phosphate synthetase from rat liver is subject to allosteric activation by *P*-Rib-*PP* and feed-back inhibition by UTP [22]. CTP synthetase from calf liver is subject to allosteric activation by GTP [23], and allosteric inhibition by the product of the reaction CTP [24]. Ribonucleotide reductase from calf thymus when reducing CDP to dCDP is subject to allosteric activation by ATP and to allosteric inhibition by dATP and to a lesser extent dTTP and dGTP [19].

If we assume that the protein concentration of the cytosol of a growing cell is approximately 25 mg/ml, then the V values for these three regulatory enzymes (Table 1) are 8.0 μM/min, 0.125 μM/min and 2.0 μM/min, respectively. The specific activity for carbamoyl phosphate synthetase from a crude cell-free extract is likely to be correct since the three enzymic activities of hOro synthetase[1] copurify in constant ratio [25], suggesting the absence of endogenous inhibitors or activators. The relatively low activities of CTP synthetase and ribonucleotide reductase *in vitro* may not relate directly to their activities *in vivo*. Cell-free extracts may contain inhibitory compounds or lack physiological activators, partial denaturation could occur during enzyme extraction, or these enzymes could be part of large multienzyme aggregates *in vivo*. Ribonucleotide reductase has been shown to be part of such a complex (replitase) during S phase of the cell cycle in Chinese hamster embryo fibroblast cells [26]. Skaper et al. [27] have reported a flux from $H^{14}CO_3^-$ into uridine phosphates of approximately 7.1 μM/min in rat liver minces and the data of Maybaum et al. [28] from mouse T-lymphoma cells are consistent with a total requirement for pyrimidines of this magnitude. Therefore carbamoyl phosphate synthetase is assumed to be the rate-limiting enzyme for the pathway (Table 1) with a normal activity of 8.0 μM/min. Parameter values listed in Table 1 have been used to simulate the interaction of *P*AcAsp with aspartate transcarbamoylase where there are time-dependent changes from an uninhibited initial steady state to a new steady state of metabolic resistance to *P*AcAsp [10]. In addition, values from Table 1 have been used to simulate progress curves for OMP and subsequent pyrimidine intermediates when BMP acts as a tight-binding inhibitor of OMP decarboxylase.

Experimental data describing the effect of 0.8 μM *P*AcAsp (a tight-binding inhibitor with a K_i of 6.2 nM) upon the aspartate transcarbamoylase reaction are shown in Fig. 1 [10]. After addition of purified hOro synthetase (0.093 μM) to a mixture of $H^{14}CO_3^-$ (3.26 mM), L-glutamine (4.0 mM), MgATP (10 mM), L-aspartate (5.0 mM), *P*-Rib-*PP* (0.1 mM) and *P*AcAsp (0.8 μM), Cbm-*P* synthesized by carbamoyl phosphate synthetase activity accumulates to levels greatly in excess of the uninhibited steady-state concentration of Cbm-*P* of 0.2 μM [10]. Fig. 1 shows that as the Cbm-*P* accumulates, so the total rate of synthesis of CbmAsp increases until a new steady-state is reached where the rate of synthesis of CbmAsp is equal to the rate of synthesis of Cbm-*P*. The final steady-state concentration of Cbm-*P* required to break the blockade by 0.8 μM *P*AcAsp is 20.5 μM (Fig. 1). The good correspondence between the experimental data points of Fig. 1 and the simulated progress curves supports the validity of our theoretical model. While the agreement is not perfect, this is due in part to the fact that the particular parameter values chosen for this simulation may vary slightly from the actual values. For example, the simulated curves are somewhat closer to the experimental data if a K_i for *P*AcAsp of 7.2 nM is used, rather than 6.2 nM as in Fig. 1. The purpose of the simulation is not to obtain a best fit to the data; rather it is to demonstrate that

[1] hOro synthetase is the trifunctional protein initiating pyrimidine biosynthesis in mammals which contains the enzymic activities carbamoyl phosphate synthetase, aspartate transcarbamoylase and dihydroorotase.

our theoretical model predicts curves of the correct general shape.

To verify further the validity of our procedures for simulating the result of interactions between a tight-binding inhibitor and its target enzyme, we now consider some experimental data obtained by Moran et al. [29] on the effect of FdUMP, a slow-binding, tight-binding inhibitor of thymidylate synthetase, in human CCRF-CEM lymphoblastic leukemia cells. They observed that after addition of 30 μM FUra, dUMP accumulated at a rate of 66 nmol/h per 10^9 cells (μM/h) after a 1-h delay and the cellular dUMP pool reached levels 300-times higher than the basal values within 11 h. They also found that measurable thymidylate synthetase activity fell to one-third of its original value over a 4-h period and then remained constant. We have simulated this system using techniques described in the theoretical section of this paper. In these experiments, the actual inhibitor (FdUMP) is not added to the cells; a precursor (FUra) is added and this is slowly converted to the active compound, presumably by endogenous orotate phosphoribosyltransferase. As a result, the total concentration of the inhibitor increases with time; Moran et al. reported that FdUMP accumulated at a rate of 0.27 μM/h after an initial lag. It is evident from their data that only free FdUMP was measured; consequently, the apparent lag in FdUMP accumulation almost certainly results from the formation of the FdUMP-thymidylate-synthetase complex. Thus, for this simulation, we assumed that FdUMP was synthesised at a rate of 0.27 μM/h without any lag. The results of this simulation (Fig. 2) yield the predictions that dUMP would rise in concentration at a rate of 69 μM/h after a 1-h delay and that measurable thymidylate synthetase activity would fall to one half of its original value over a 4-h period and thereafter remain constant. These predictions are in good agreement with the experimental observations illustrated in Fig. 5A of [29] by Moran et al. who have concluded that FdUMP does not give stoichiometric inhibition of thymidylate synthetase in CCRF-CEM cells due to competition for binding of FdUMP to thymidylate synthetase by high concentrations of accumulated dUMP. Thus metabolic resistance appears to be an important consideration for the interaction of FdUMP with thymidylate synthetase *in vivo* (Fig. 2) as it is for the *P*AcAsp/aspartate transcarbamoylase system *in vitro* (Fig. 1). Having established the validity of our simulation techniques by comparison with experimental data (Fig. 1 and 2), a detailed simulation was performed for a hypothetical system where BMP, a slow-binding, tight-binding inhibitor of OMP decarboxylase ($K_i = 8.8$ pM, $k_4 = 3.5 \times 10^{-3}$ min^{-1} [30]) was added to a system *in vivo*.

In order to simulate the section of the pyrimidine pathway from OMP to DNA, it should be recalled that OMP is a precursor of all of the pyrimidine nucleotides. For example, UDP is converted to both UTP and dUDP and the latter compound is ultimately converted to the dTTP needed for DNA synthesis. In a similar way, UTP partitions between incorporation into RNA and conversion to CTP which can be converted to CDP or incorporated into RNA. Thus, while OMP is formed at a rate of 8.0 μM/min, only a fraction of it is converted to dCDP which is committed to DNA synthesis. Maybaum et al. [28] have calculated the rates of incorporation of CTP into RNA and of dCTP and dTTP into DNA for a mouse cell line. While they did not report a rate for the incorporation of UTP into RNA, we assume that it would be similar to that of CTP. We therefore partitioned the total flux of 8.0 μM/min in the same relative proportions as those reported by Maybaum et al. The resulting fluxes

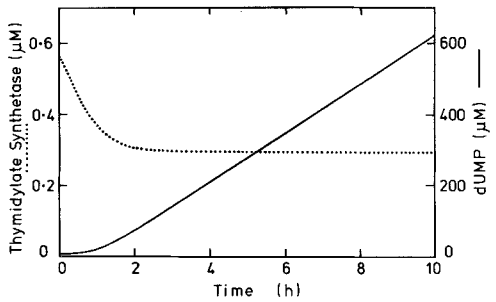

Fig. 2. *Simulation of progress curves for dUMP and active thymidylate synthetase after addition of 30 μM FUra.* The simulation was performed using the following parameter values [3]: initial dUMP concentration, 5 μM; apparent Michaelis constant for dUMP, 2.8 μM; total concentration of thymidylate synthetase, 0.57 μM [29] (assuming 10^9 cells is equivalent to a volume of 1 ml); first-order rate constant for dissociation of the thymidylate-synthetase-FdUMP complex, 0.03 min^{-1} [3]; inhibition constant for FdUMP, 11.1 nM [3]; and a constant rate of synthesis of FdUMP of 0.27 μM/h. Details are described in the theoretical section of this paper

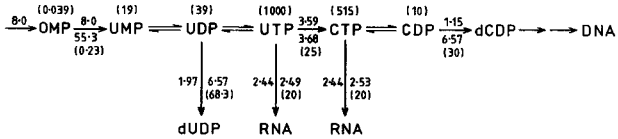

Fig. 3. *Simplified pyrimidine pathway.* Intermediates connected by double arrows were assumed to be maintained at chemical equilibrium. The concentrations (μM) of each intermediate in the absence of BMP are shown in parentheses above the relevant compound. The ratio of CTP:CDP was maintained at 515:10 as the concentration of the total cytidine phosphates pool varied. In a similar way, UMP:UDP:UTP was maintained at 19:39:1000. The non-equilibrium steps are shown by single arrows and the fluxes through such steps (μM/min) are indicated by the number above or to the left of the arrow. The numbers below or to the right of these non-equilibrium steps represent the maximum velocity (μM/min) and Michaelis constant (μM) of the enzyme involved, with the latter value being shown in parentheses. In all cases except OMP decarboxylase and ribonucleotide reductase, the maximum velocity was calculated so as to be consistent with the flux, the Michaelis constant and the substrate concentration, assuming simple Michaelis-Menten kinetics. For OMP decarboxylase, the steady-state concentration of OMP was calculated from the flux (8.0 μM/min), the maximum velocity and the Michaelis constant (Table 1). For ribonucleotide reductase, which catalyses the formation of dUDP and dCDP, the maximum velocity and the Michaelis constant for UDP were calculated from the fluxes, the concentrations of UDP and CDP, and the Michaelis constant for CDP assuming alternative substrate inhibition

(UTP→RNA, 2.44 μM/min; CTP→RNA, 2.44 μM/min; dCTP→DNA, 1.15 μM/min; and dTTP→DNA; 1.97 μM/min) are shown in Fig. 3.

It is evident from Table 1 that certain enzymes are present in a vast excess to that required to maintain the fluxes indicated in Fig. 3. For example, nucleoside diphosphate kinase, which converts UDP to UTP, has a maximum velocity of 110000 μM/min while the net flux through this reaction is only 6.03 μM/min. Since the cellular concentration of UDP is 39 μM and the Michaelis constant for this substrate is probably in the region of 200 μM, the expected flux is 17950 μM/min which is nearly 3000 times the net flux, Clearly, the interconversion of UDP and UTP is at chemical equilibrium and will remain so unless the flux is vastly increased. Since

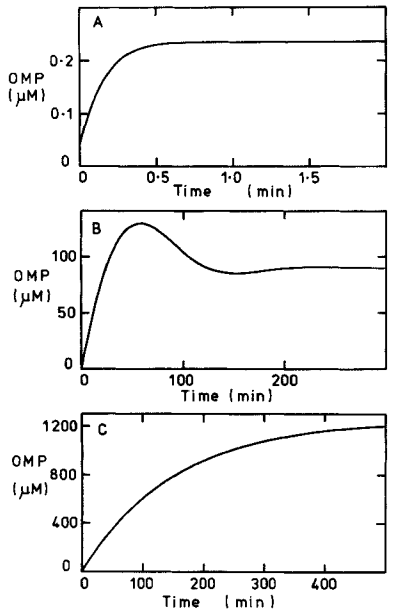

Fig. 4. *Effect of BMP on the accumulation of OMP.* The simulations were performed using the simplified pyrimidine pathway described in Fig. 3. BMP was assumed to be a slow-binding, tight-binding inhibitor ($K_i = 8.8\,\text{pM}, k_4 = 3.5 \times 10^{-3}\,\text{min}^{-1}$) of OMP decarboxylase which was present at a concentration of 0.14 μM. Concentrations of BMP were (A) 0.1 μM, (B) 0.14 μM; and (C) 0.4 μM

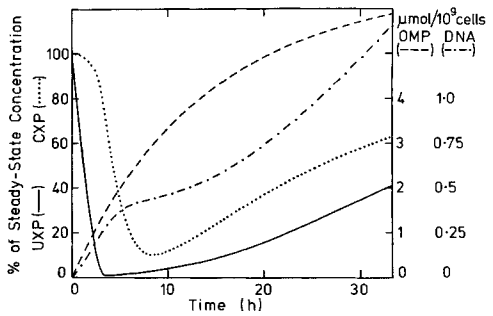

Fig. 5. *Effect of 1.6 μM BMP on the concentrations of UXP and CXP, and on the accumulation of OMP and DNA.* Conditions were as described in Fig. 4. The concentrations of the uridine phosphates (U*X*P, ——) and the cytidine phosphates (C*X*P, ····) are expressed as a percentage of the steady-state concentrations. OMP (– – – –) and DNA (–·–·–·–) are expressed as μmol/10^9 cells

the addition of BMP can only decrease the flux, it was assumed that UDP and UTP remain in equilibrium at all times and are maintained in the relative ratio of 39:1000, the steady-state ratio. Similar arguments led to the conclusion that UMP and UDP are maintained in the ratio 19:39 and that CTP:CDP remains at 515:10. For all other reactions except those catalysed by ribonucleotide reductase, the maximum velocity of the enzyme concerned was calculated so that it was just sufficient to maintain the flux through that reaction, given the known steady-state concentration and Michaelis constant for the substrate. The appropriate values are also shown in Fig. 3.

Ribonucleotide reductase, which catalyses the conversion of both UDP and CDP to the corresponding deoxynucleoside diphosphates, is a special case. Since there are two possible substrates competing for the same enzyme, UDP will inhibit CDP reduction and vice versa. In this situation (alternative substrate inhibition) the inhibition constant of each compound will be equal to its own Michaelis constant.

Fig. 4 shows the effect of several BMP concentrations on the accumulation of OMP. At a BMP concentration of 0.1 μM which is below that of OMP decarboxylase (0.14 μM, Fig. 4A) a rather small accumulation of OMP is required to reverse the inhibition and OMP stabilizes to a new steady-state concentration within 1 min. By contrast, a BMP concentration of 0.4 μM, somewhat greater than that of the enzyme (Fig. 4C), causes a massive accumulation of OMP which continues over several hours. This dramatic change in the final steady-state concentration for just a fourfold change in the inhibitor concentration is characteristic of metabolic resistance to tight-binding inhibitors [3].

An interesting situation occurs when the concentration of BMP is in the range 0.125 – 0.2 μM which is approximately equal to, or slightly greater than, the enzyme concentration; there is a marked 'overshoot' in OMP accumulation and the concentration eventually stabilizes at the new steady-state after a series of progressively smaller oscillations (Fig. 4B). This phenomenon is a direct result of the fact that BMP is a slow-binding inhibitor; OMP is accumulating at a rate which is faster than the interconversion of free enzyme and the enzyme-inhibitor complex can adjust to the changing substrate concentration.

The addition of BMP causes a transient decrease in the concentrations of the uridine phosphates pool (U*X*P) and the cytidine phosphates pool (C*X*P), and a temporary reduction in the rate of DNA synthesis. These effects, and particularly those on C*X*P and DNA, are not substantial at BMP concentrations below 0.2 μM. The principal reason for this is that when the conversion of OMP to UMP is inhibited, there remains a large pool of uridine phosphates which is depleted only slowly. Meanwhile, OMP is accumulating and thereby restoring UMP synthesis. For example, at 0.2 μM BMP, UTP never falls below 675 μM which is 27-times the Michaelis constant of CTP synthetase for this substrate; hence, there will be very little interruption of the production of CTP.

At concentrations of BMP above 0.5 μM, the effects on U*X*P are marked, while C*X*P and DNA are also affected. This is illustrated for 1.6 μM BMP in Fig. 5. At this concentration of the inhibitor, there is a substantial accumulation of OMP which has reached 5.71 mM after 30 h. The concentration of the uridine phosphates falls dramatically, reaching a minimum of 1% of the steady-state concentration after 4 h; thereafter the U*X*P pool recovers. The cytidine phosphates also fall after a brief delay, reaching a minimum of 11% after 8 – 9 h, followed by a slow recovery. When C*X*P falls below 30% of the steady-state concentration, DNA synthesis is markedly affected and as the C*X*P pool recovers, so too does DNA synthesis.

Eventually, DNA synthesis is restored to the uninhibited rate and, if a tangent is drawn to the curve, the point at which this tangent crosses the abscissa may be considered to represent the delay in mitosis which is elicited by this concentration of BMP. We have estimated this mitotic delay for a range of BMP concentrations and these results are shown in Fig. 6. Low BMP concentrations have little effect; for example, 0.3 μM BMP causes a mitotic delay of 40 min. Between 0.3 μM and 2 μM BMP it rises to a little over 20 h. Above 2 μM BMP, there is approximately linear dependence, with each additional 1 μM BMP causing a further delay of a little over 10 h. To put these figures in perspective, the deoxycytidine content of mouse DNA is 4.79 μmol/10^9 cells [28] and at the uninhibited rate of dCDP synthesis of

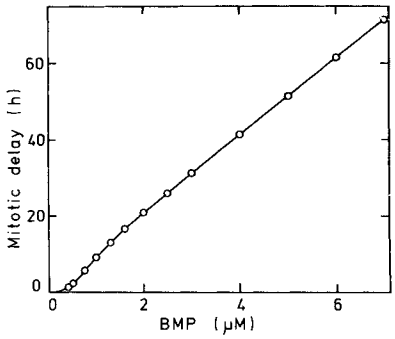

Fig. 6. *Effect of BMP on the mitotic delay.* A series of DNA accumulation curves, over a range of BMP concentrations, were calculated as described in Fig. 5. These simulations were continued until the rate of DNA synthesis recovered to the steady-state rate. A tangent was drawn to the curve and projected back to the abscissa to yield the mitotic delay which was plotted against the concentration of BMP

1.15 μM/min the doubling time would be 69.5 h. Since 6.8 μM BMP causes a mitotic delay of 69.5 h, this concentration of the inhibitor would halve the growth rate.

It is clear that when the pyrimidine pathway is blocked by a tight-binding inhibitor, this blockade can eventually be broken by accumulation of the substrate of the inhibited enzyme. However, prolonged depletion of a vital precursor for synthesis of DNA may prove to be fatal to a cell before substrate can accumulate to levels sufficient to give rise to metabolic resistance. From the correlation of the rate of DNA synthesis with the level of the dCTP pool in the Chinese hamster ovary cells, Bjursell and Reichard [7] have proposed that the size of the dCTP pool may have a regulatory function for the rate of DNA synthesis. In addition, Reynolds et al. [8] have proposed that a critical concentration of dCTP of about 32 μM is required for the maintenance of normal rates of DNA synthesis in mouse lymphoma and myeloma cell lines. However, it would seem that a critical threshold concentration of dCTP can only be proposed for cell lines which have approximately the same growth rate and content of deoxycytidine in their DNA. Indeed, Walters and Ratliff [31] have proposed that reduction of any of the four deoxyribonucleoside triphosphate pools below a critical level will inhibit DNA synthesis. In our view, the extent to which mitosis is delayed might be the crucial factor in the toxicity of an inhibitor of nucleotide biosynthesis; if this is sufficiently prolonged then cell death will result. It follows that a slow growing cell would be less susceptible to the effects of BMP than a rapidly growing cell. This is the basis for the selective toxicity of tight-binding inhibitors of nucleic acid biosynthesis for rapidly growing tumour cells.

These proposals should be testable experimentally for a particular cell line and pyrimidine pathway inhibitor. Indeed at an inhibitor concentration sufficient to cause cell death it should be possible to 'rescue' the cells by addition of the appropriate nucleoside to the growth medium. Such a rescue technique has been succesfully used on cancer patients being treated with methotrexate [4]. Tight-binding inhibition of dihydrofolate reductase by methotrexate results in depletion of intracellular reduced folates required for the biosynthesis of thymidylate and inosinate, essential precursors of nucleic acids. Protection of patients against myelosuppression by methotrexate can be achieved by infusion of thymidine alone because of high endogenous concentrations of hypoxanthine in bone marrow [32].

This work was supported in part by National Health and Medical Research Council project grant 830672 to R. I. C. during tenure of a C. R. Roper Fellowship in Medical Research. We thank Dr T. W. Traut for supplying some of the information in Table 1.

REFERENCES

1. Montgomery, J. A. (1979) *Methods Cancer Res. 16*, 3–41.
2. Morrison, J. F. (1982) *Trends Biochem. Sci. 7*, 102–105.
3. Christopherson, R. I. & Duggleby, R. G. (1983) *Eur. J. Biochem. 134*, 331–335.
4. Howell, S. B., Herbst, K., Boss, G. R. & Frei, E. (1980) *Cancer Res. 40*, 1824–1829.
5. McCracken, D. D. & Dorn, W. S. (1964) *Numerical Methods and FORTRAN Programming*, John Wiley and Sons, New York.
6. Chandler, J. P., Hill, D. E. & Spivey, H. O. (1972) *Comput. Biomed. Res. 5*, 515–534.
7. Bjursell, G. & Reichard, P. (1973) *J. Biol. Chem. 248*, 3904–3909.
8. Reynolds, E. C., Harris, A. W. & Finch, L. R. (1979) *Biochim. Biophys. Acta 561*, 110–123.
9. Selkurt, E. E. (1968) in *Metabolism* (Altman, P. L. & Dittmer, D. S., eds) p. 536, Federation of American Societies for Experimental Biology, Bethesda, MD.
10. Christopherson, R. I. & Jones, M. E. (1980) *J. Biol. Chem. 255*, 11381–11395.
11. Jones, M. E. (1980) *Annu. Rev. Biochem. 49*, 253–279.
12. Hitchings, G. H. (1973) *Adv. Enzyme Regul. 12*, 121–129.
13. Traut, T. W., Payne, R. C. & Jones, M. E. (1980) *Biochemistry 19*, 6062–6068.
14. Hunting, D., Hordern, J. & Henderson, J. F. (1981) *Can. J. Biochem. 59*, 838–847.
15. Maness, P. F. & Orengo, A. (1976) *Cancer Res. 36*, 2312–2316.
16. Payne, R. C. & Traut, T. W. (1982) *Anal. Biochem. 121*, 49–54.
17. Agarwal, R. P., Robison, B. & Parks, R. E., Jr (1978) *Methods Enzymol. 51*, 376–386.
18. McPartland, R. P. & Weinfeld, H. (1976) *J. Biol. Chem. 251*, 4372–4378.
19. Eriksson, S., Thelander, L. & Akerman, M. (1979) *Biochemistry 18*, 2948–2952.
20. Cory, J. G. & Mansell, M. M. (1975) *Cancer Res. 35*, 390–396.
21. Reference deleted.
22. Mori, M., Ishida, H. & Tatibana, M. (1975) *Biochemistry 14*, 2622–2630.
23. Savage, C. R. & Weinfeld, H. (1970) *J. Biol. Chem. 245*, 2529–2535.
24. McPartland, R. P. & Weinfeld, H. (1979) *J. Biol. Chem. 254*, 11394–11398.
25. Coleman, P. F., Suttle, D. P. & Stark, G. R. (1977) *J. Biol. Chem. 252*, 6379–6385.
26. Noguchi, H., Reddy, G. P. V. & Pardee, A. B. (1983) *Cell 32*, 443–451.
27. Skaper, S. D., O'Brien, W. E. & Schafer, I. A. (1978) *Biochem. J. 172*, 457–464.
28. Maybaum, J., Cohen, M. B. & Sadee, W. (1981) *J. Biol. Chem. 256*, 2126–2130.
29. Moran, R. G., Spears, C. P. & Heidelberger, C. (1979) *Proc. Natl Acad. Sci. USA 76*, 1456–1460.
30. Levine, H. L., Brody, R. S. and Westheimer, F. H. (1980) *Biochemistry 19*, 4993–4999.
31. Walters, R. A. & Ratliff, R. L. (1975) *Biochim. Biophys. Acta, 414*, 221–230.
32. Howell, S. B., Mansfield, S. J. & Taetle, R. (1981) *Cancer Res. 41*, 945–950.

R. G. Duggleby, Department of Biochemistry, University of Queensland, Saint Lucia, Brisbane, Queensland, Australia 4067

R. I. Christopherson, Department of Biochemistry, University of Melbourne, Parkville, Victoria, Australia 3052